JOURNAL OF MATERIALS SCIENCE 14 (1979) 431–442

The debonding and pull-out of ductile wires from a brittle matrix

J. BOWLING*, G. W. GROVES
Department of Metallurgy and Science of Materials, Oxford University, UK

An experimental investigation into the debonding and pull-out of nickel wires from epoxy resin and cement paste matrices has been carried out. Above a critical embedded length both the debonding and pull-out stresses attain limiting values. A theory based on the model of a yielded zone travelling up the wire behind a debonding front was shown to describe the observed dependence of the limiting debonding stress on the yield stress, diameter and surface roughness of the wire. Pull-out behaviour subsequent to debonding was explained using this model in terms of an unyielded plug at the end of the wire. Orientation of the wire to the loading direction was found to raise the limiting debonding and pull-out stresses due to enhanced friction at the wire exit point.

1. Introduction

In a previous paper [1] it was reported that ductile metal wires embedded in a brittle matrix would in certain cases debond and pull out of the matrix at a stress somewhat in excess of their initial tensile yield stress, no matter how large the length of wire embedded. The interest of this observation lies in the possibility which it offers of producing a large resistance to the propagation of a crack in a brittle matrix composite by incorporating metal wires which bridge the crack faces and exert their yield stress as a closure stress upon the crack. In this way the fracture toughness of the material would be enhanced in a predictable way. A significant feature of the observed behaviour was that pull-out stresses of the order of the yield stress of the wire could be maintained as the crack developed very large openings. This would be important in increasing the resistance to the propagation of cracks in specimens of such a geometry that large crack openings occur (e.g. a bending or a double cantilever beam (DCB) geometry) and also in increasing the resistance of the material to catastrophic disintegration. The materials investigated were an epoxy resin and, to a lesser extent, cement paste, incorporating nickel wires. These are model materials; the material of this general type of which most practical use has so far been made is cement or concrete reinforced with steel wire. In this paper we shall consider the extent to which a practical material might make use of the effect described above. To answer this question, a more detailed understanding of the effect itself is required. In the earlier work [1] the importance of the radial plastic contraction of the wire at its tensile yield stress in taking its surface out of contact with the matrix was recognised. Thus the limiting pull-out stress would be determined by that stress which would produce the plastic strain needed to give the somewhat rough surface of the wire clearance from the matrix. In this paper we develop a detailed model for the debonding and pull-out processes and examine the effects on debonding and pull-out of the yield stress, surface roughness, diameter, embedded length and orientation of the wire. The experiments from which the model was developed were carried out on pre-cracked single- or double-wire specimens of nickel wire embedded in epoxy resin or cement paste. In a subsequent paper it will be shown that in multi-wire SEN or DCB fracture toughness specimens of these materials precisely the same debonding and pull-out effects occur as are observed in the simplest single-wire specimens

*Present address: I.M.I. Ltd, Kynoch, Birmingham, UK.

and that the fracture behaviour of the multi-wire fracture toughness specimen can be predicted from the observations on single wires reported here. In order to give as coherent a presentation of the results as possible, a model for the debonding and pull-out processes will be described first. The experimental results which confirm and amplify the details of this model will then be presented, followed by a discussion of the possible application of the effects observed in practical composites.

2. Model for the debonding and pull-out of a ductile wire

The model is illustrated in Fig. 1, which shows the various stages of debonding and pull-out and the corresponding points on the load–displacement plot for the withdrawal of an embedded wire. It is assumed that the initial debonding stress is less than the yield stress of the wire. There are two theoretical treatments of the debonding stress. One, due to Outwater and Murphy [2], uses an energy balance argument similar to the Griffith theory of brittle fracture to predict a debonding stress, σ_d:

$$\sigma_d = \sqrt{\left(\frac{8E\gamma}{r}\right)}, \qquad (1)$$

where E is the Young's modulus of the fibre or wire, r is its radius and γ the fibre–matrix interfacial energy. The second approach is to use shear lag theory to determine the distribution of shear stress at the fibre–matrix interface and to say that debonding occurs when the maximum value of this shear stress reaches a critical value [3, 4]. The difficulty with this approach is that we observe in stress birefringence studies that there is a stress concentration at the debonding front, which is unlikely to be predicted accurately by shear lag analysis. However, the choice of the theoretical approach to debonding does not strongly affect the model. An important feature of the model is that the shear stress is still transmitted across the debonded region of the interface behind the debonding front so that initially an increasing stress on the wire is required to propagate the debonding front. Thus, according to Outwater and Murphy [2];

$$\sigma_d = \sqrt{\left(\frac{8E\gamma}{r}\right) + \frac{2\tau x}{r}}, \qquad (2)$$

where τ is the interfacial shear stress, assumed to be constant in the debonded region, and x is the debonded length. At a sufficiently large value of x, the debonding stress exceeds the yield stress of the wire. The relatively large plastic radial contraction of the wire then reduces the interfacial shear stress to zero. The debonding front continues to propagate with a constant stress applied to the wire at

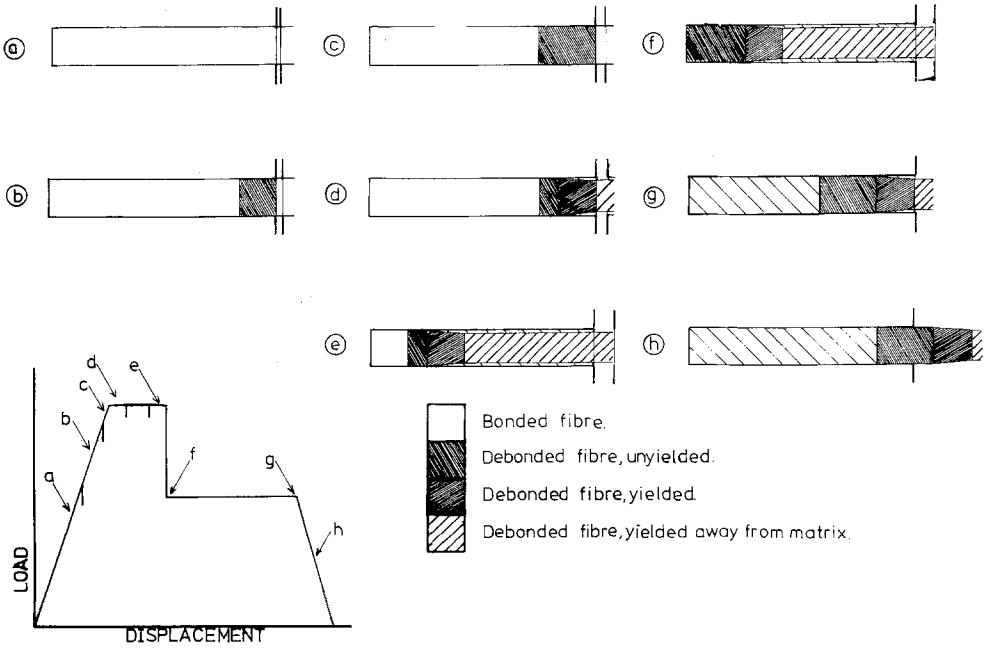

Figure 1 Schematic representation of debonding and pull-out of a ductile wire from a brittle matrix.

this stage. (In practice the debonding front usually propagates in small jumps rather than smoothly, accompanied by the small load drops which are shown on the load–displacement curve.) This produces a "debonding plateau" in the load–displacement curve. The magnitude of the plateau debonding stress is determined by the plastic strain needed to remove the interfacial shear traction. This depends critically upon the small-scale roughness of the wire surface. The profile of an actual wire surface as obtained with a Talysurf is shown in Fig. 2. Since the plastically straining wire undergoes a substantial longitudinal displacement with respect to the matrix, the radial contraction required to give clearance is the height between nearby hills and valleys in the surface profile, shown as X in Fig. 2. The longitudinal strain required, ϵ, if predominantly plastic, is twice the radial strain. Thus for a wire of diameter d,

$$\epsilon = \frac{4X}{d}. \tag{3}$$

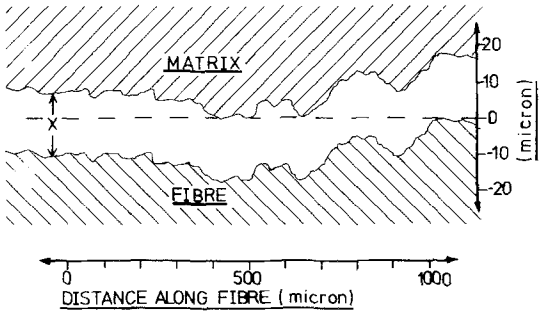

Figure 2 Profile of a fibre–matrix interface.

It is difficult to assign a precise value to X from profiles of the wire surface because of the difficulty of deciding the distance along the wire over which the maximum height difference should be taken. Some additional contribution to X may be required to overcome a radial compressive elastic strain in the matrix arising from the thermal expansion mismatch of the wire and matrix on cooling from the curing temperature. Part of this mismatch would be expected to be relieved by plastic flow in the matrix. The total mismatch strain is estimated to be 0.4%; if none of this were relieved by plastic flow it would still only account for about half the observed strain in our smoother wires. The extent of the debonding plateau D, is given by

$$D = \epsilon(l - l_k) \tag{4}$$

where l is the total length of wire and $l_k/2$ is the minimum length of wire remaining in contact with the matrix, at either end of the wire, which will support the debonding stress. (We assume a wire embedded with equal lengths $l/2$ on either side of the crack which debonds on both sides symmetrically.) The displacement D added to a small elastic displacement would then give the crack opening needed to fully debond the wire. The total length l_k remaining in contact with the matrix at the wire ends has an alternative interpretation as the length of wire which must be exceeded in order to obtain a debonding plateau. We may term this the critical length. The debonding plateau stress σ_p is the flow stress at the strain ϵ; since in our case ϵ will be usually several per cent, the debonding plateau stress will usually only modestly exceed the yield stress of the wire, given the relatively low work-hardening rate of our wires.

The shear stress supported by the bonded fibre will usually exceed the shear stress transmitted after debonding so that in this case a load drop will occur at the commencement of pull-out. (However, the pull-out stress can be similar in magnitude to the debonding plateau stress – by coincidence this was the case in an earlier paper [1] where it led to difficulty in distinguishing the debonding and pull-out stages.) Generally pull-out occurs from one side only of the crack so that the pull-out process is the withdrawal of a "plug" at one end of the wire. The length of this plug will be the same as the length at one end of the wire in contact with the matrix at the moment of final debonding, $l_k/2$. Until the beginning of the plug reaches the crack surface (Fig. 1g) the pull-out load remains constant. The debonding plateau is therefore followed by a pull-out plateau.

3. Experimental details

Initially, two-wire composites were fabricated from nickel wire and epoxy resin, as described in previous papers [1, 5]. These specimens were used for testing the effects of wire yield stress and wire roughness on the debonding plateau stress (see Section 4.1). However, it was found that the process of debonding and pull-out could be better followed and identified with different stages of the load–displacement curve by using single-wire specimens, and these were used for all further investigations. The wires were located in slots machined in a resin blank into which the same resin was cast. The crack was simulated by a mica

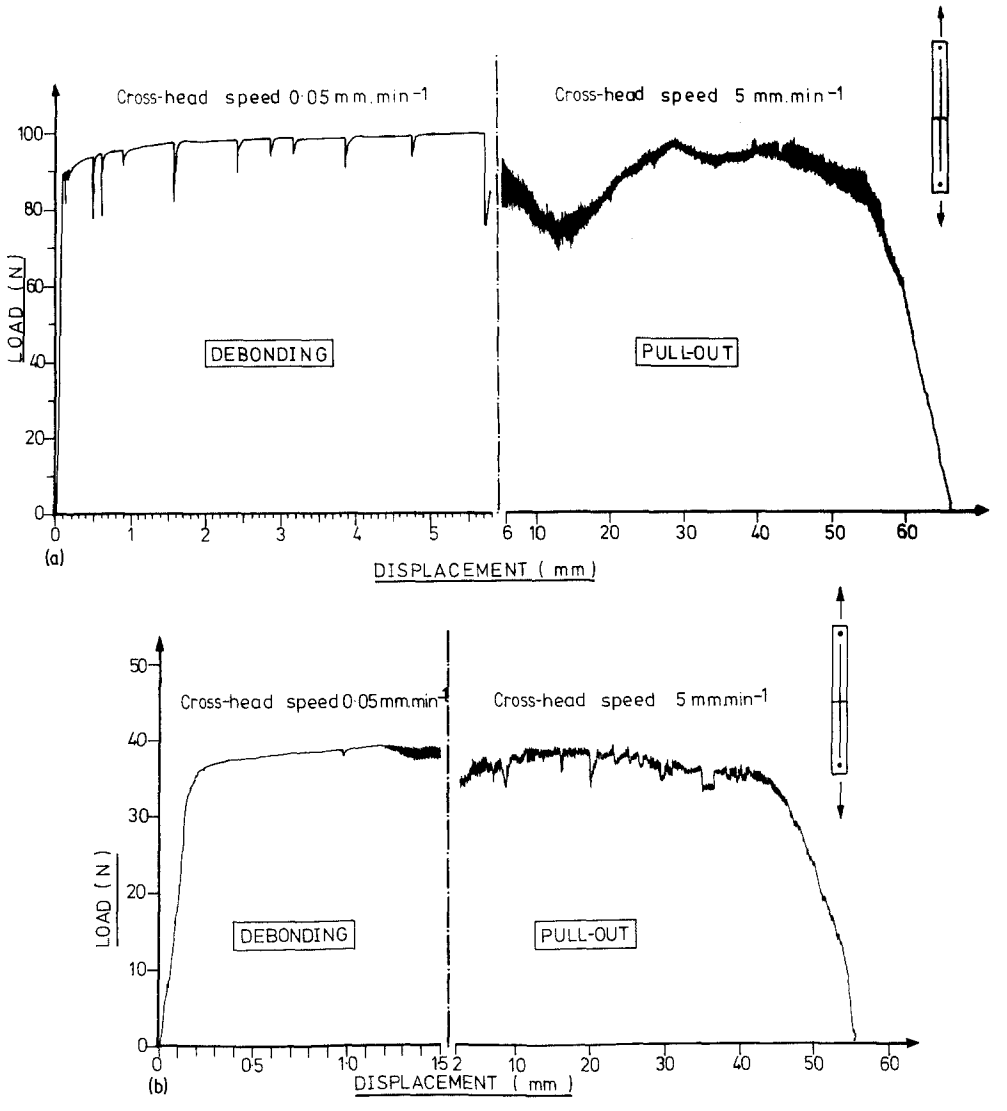

Figure 3 Load–displacement curves for the debonding and pull-out of nickel wires, (a) and (c) resin matrix, (b) and (d) cement matrix.

sheet through which the wire passed, as described previously [1, 5]. The mica sheet was positioned at the mix-point of the wire so that equal lengths of wire were embedded on either side of the "crack". The epoxy resin used for the double-wire specimens and for the diameter dependence studies (Sections 4.1 and 4.2) was Araldite MY753 with hardener HY956. For the embedded length and orientation studies (Sections 4.3 and 4.5) Araldite MY753 was used with hardener HY951. This second resin had been found to be more convenient for fabricating multi-wire specimens. The change in resin type had no significant effect in the experiments reported here.

Cement matrix specimens were made by casting the cement round the wire which was located in a slot in a resin blank. The slot had irregular sides so that the cement was mechanically keyed into place. The cement (ordinary Portland) had a water-to-cement ratio of 0.3 and was cured under water at 50° C for 14 days. The specimen was kept wet prior to and during testing.

4. Results

4.1. Load–displacement curves and photoelastic observations

A load–displacement curve in a case where the load drop at the end of debonding is relatively small is shown in Fig. 3a. The debonding plateau stress is nearly always constant, apart from the

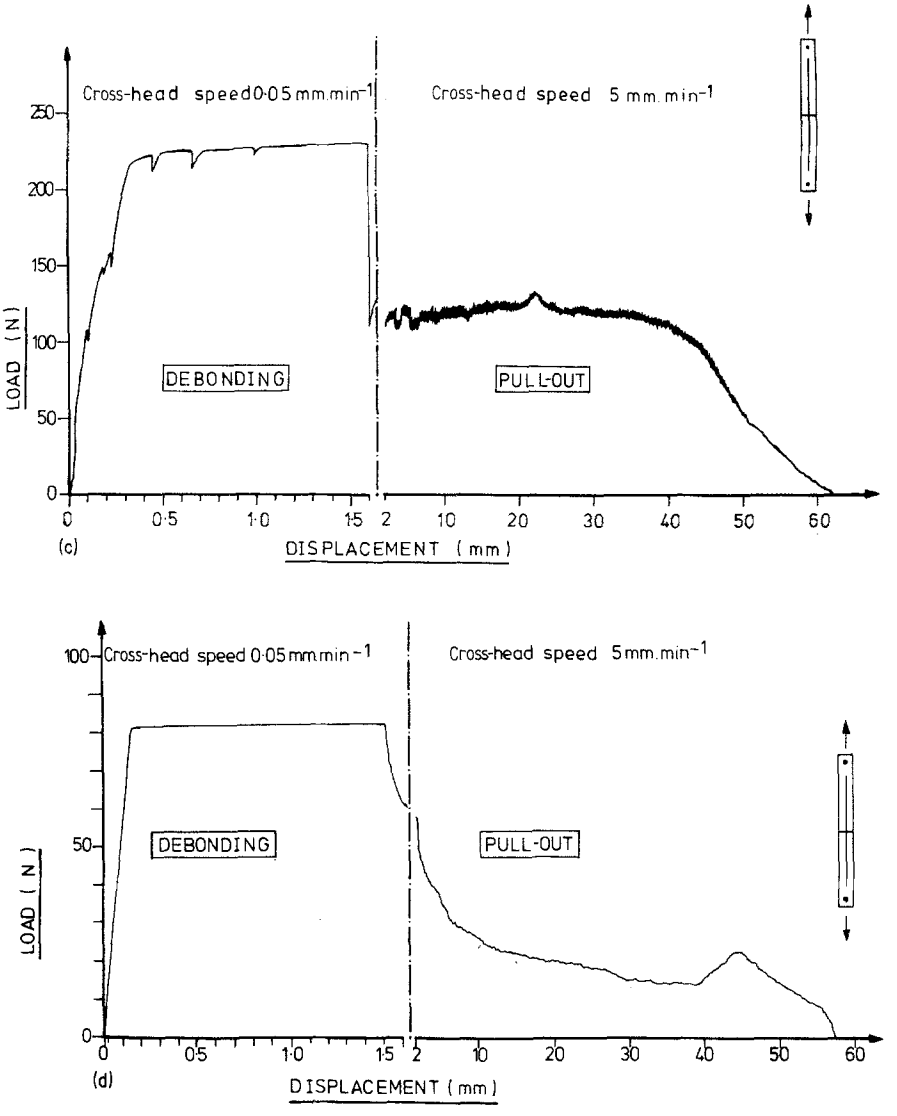

Figure 3 continued.

small load drops accompanying advances of the debonding front. The fluctuations in pull-out stress on the fine scale are due to stick-slip motion of the wire, and on the larger scale, are presumably due to variations in wire diameter such that the "plug" at the end of the wire is drawn through a matrix tunnel of slightly varying diameter. These fluctuations in stress appear to be random and are always present although often to a less marked extent than is shown in Fig. 3a. A similar form of curve was obtained for a cement matrix, as shown in Fig. 3b, when the wire yield stress was $250\,MN\,m^{-2}$. In many other cases the pull-out stress was substantially lower than the debonding plateau stress, as in Fig. 3c and d.

In a resin matrix, the position of the debonding front could be seen by greater reflectivity of the debonded interface, confirming that the initial load plateau does correspond to the propagation of debonding along the wire. The presence of a plug at the end of the wire during pull-out could be confirmed by photoelastic observation, which also showed the sharp stress fluctuations at the plug–resin interface, presumably arising from the irregularities on the wire surface (Fig. 4). It was also possible to confirm by photoelastic observation that during debonding a stress acts on the debonded interface behind the debonding front. The observed load–displacement curves and photoelastic observations therefore confirmed the broad outlines of the model.

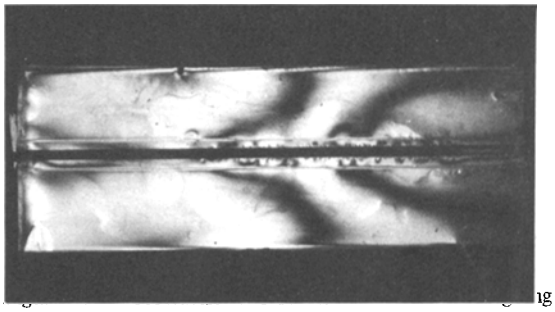

pull-out.

4.2. Effect of wire yield stress and wire roughness

As-received nickel wire was pulled to flow stresses of 265 and 400 MN m^{-2} and double wire specimens with an epoxy resin matrix (MY753 HY956) were tested. To compare these results with the behaviour of rougher wire, specimens with the same wire pulled to fracture, annealed and pulled to flow stresses of 235 and 400 MN m^{-2} were tested. Talysurf measurements and scanning electron microscope observations of the surface of this wire confirmed that pulling to failure had substantially increased its roughness. Fig. 5a and b shows the increase in debonding plateau stress obtained by roughening the surface of the wire. In the case of the 400 MN m^{-2} yield stress, the UTS of the rough wire was reached before debonding could propagate fully and the wire fractured.

The pull-out stress is also affected by the roughness of the wire, being approximately 300 MN m^{-2} for the 235 MN m^{-2} yield stress rough wire and 150 MN m^{-2} for the 265 MN m^{-2} yield stress smooth wire. The pull-out stress is increased more than the debonding stress by roughness so that the rougher wire shows the smaller load drop on termination of debonding.

4.3. Effect of wire diameter

This was investigated with single-wire specimens of nickel wire with diameters in the range 0.5 to 1.6 mm. The wire was prepared by cold-drawing in the laboratory followed by annealing under argon + 2% hydrogen and pulling to a yield stress of 400 MN m^{-2}. The matrix was epoxy resin (MY753 HY956).

The plateau debonding stress increases slowly as the wire diameter is reduced (Fig. 6). The extent of the debonding plateau increases much more markedly (Fig. 7), showing that the essential effect of reducing the wire diameter is to increase the plastic strain associated with debonding.

The result shown in Fig. 7 can be derived from Equations 3 and 4 of the model. Thus

$$D = \frac{4X}{d}(l - l_k). \tag{5}$$

The length in contact with the matrix at each end of the wire, $l_k/2$, can be derived from a balance of forces on the wire at the instant of final debonding.

$$l_k = \frac{\sigma d}{2\tau_{av}}, \tag{6}$$

where σ is the debonding plateau stress and τ_{av} the

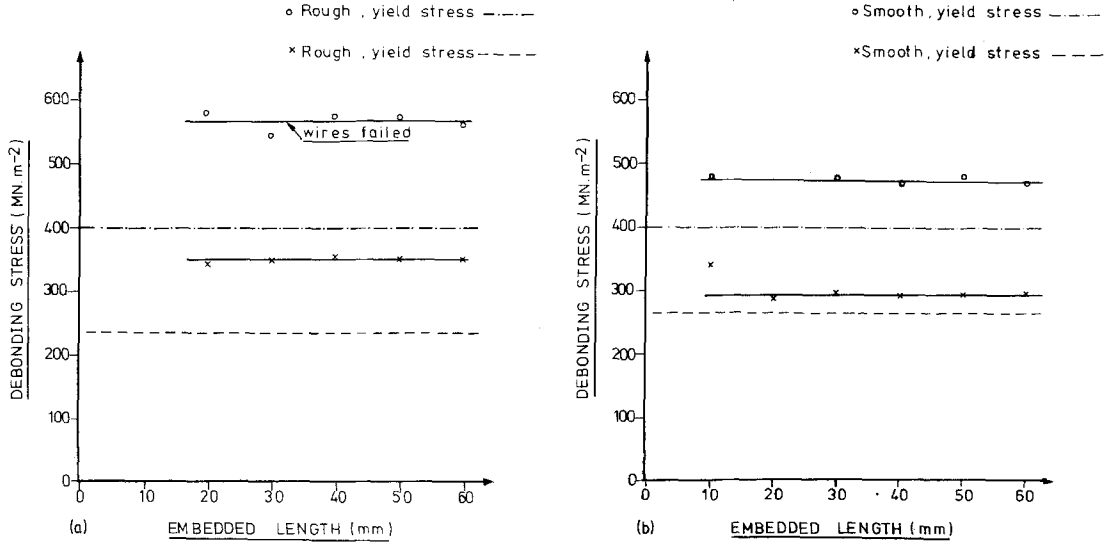

Figure 5 Debonding stresses for (a) rough and (b) smooth wires.

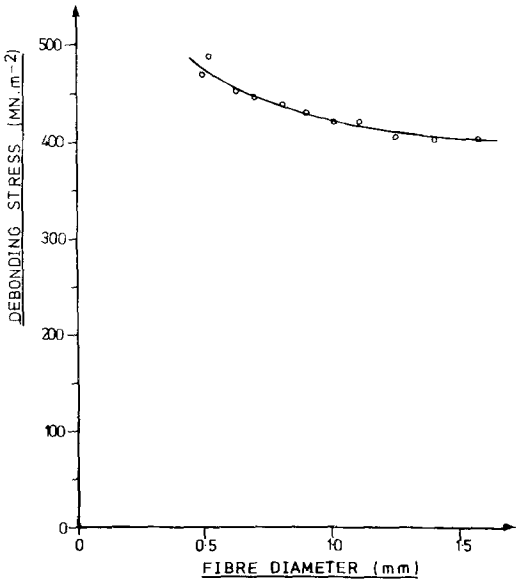

Figure 6 Dependence of debonding stress on wire diameter. Yield stress 400 MN m^{-2}.

average shear stress over the length $l_k/2$. Since σ is observed to vary only slowly with d (Fig. 6), then assuming τ_{av} is likewise independent of d, Equation 5 can be written

$$D = \frac{4Xl}{d} - \alpha, \qquad (7)$$

where $\alpha = 2X\sigma/\tau_{av}$ is nearly independent of d, for a set of wires having the same surface condition and therefore the same value of X.

The slope of the straight line in Fig. 7 gives a value of X of 10 μm. It is difficult to make a precise comparison of this value with direct observations of surface roughness, because of the problem of not knowing the scale of distance along the wire over which surface fluctuations should be measured, but it is clearly of a reasonable magnitude since Talysurf measurements of the drawn wire showed surface fluctuations of several microns. The plastic strain associated with debonding which is implied by this value of X is 8% for the 0.5 mm diameter wire, for example. The sensitivity of the relationship between debonding plateau and wire diameter to surface finish was confirmed by additional tests on a set of wires of different as-received diameters, pulled to a yield stress of 400 MN m^{-2}.

Talysurf traces indicated a smoother finish to this wire than to the laboratory-drawn wire and they also showed a tendency for the roughness of

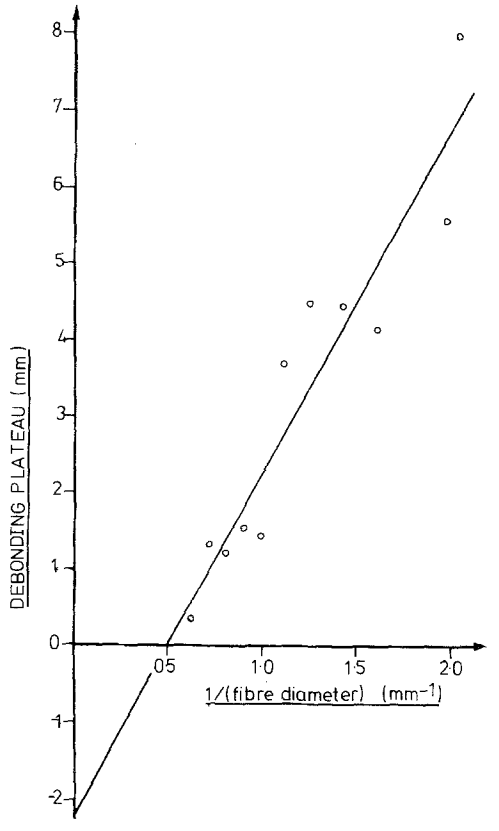

Figure 7 Dependence of length of debonding plateau on wire diameter.

the as-received wire to increase with increasing diameter. The debonding stress and debonding plateau lengths nevertheless showed similar trends with fibre diameter to the laboratory drawn wire but with slightly lower debonding stresses and much shorter debonding plateau.

The intercept of the line in Fig. 7 gives a value of l_k/d, the critical aspect ratio, of 56, and a corresponding value of τ_{av} of 3.6 MN m^{-2}. The value of $l_k/2d$ is an estimate of the plug length to diameter ratio and this was in good agreement with photoelastic observations of the plug during pull-out.

4.4. Effect of embedded length

Wires received in two diameters, 0.5 and 1 mm were pulled to a 400 MN mm^{-2} yield stress and single-wire specimens with a range of embedded lengths were tested. The variation of the debonding stress, defined as the maximum stress up to completion of debonding, is shown in Fig. 8a and b. The debonding stress is slightly higher for the smaller diameter, as expected from the results of the previous section. The critical embedded length

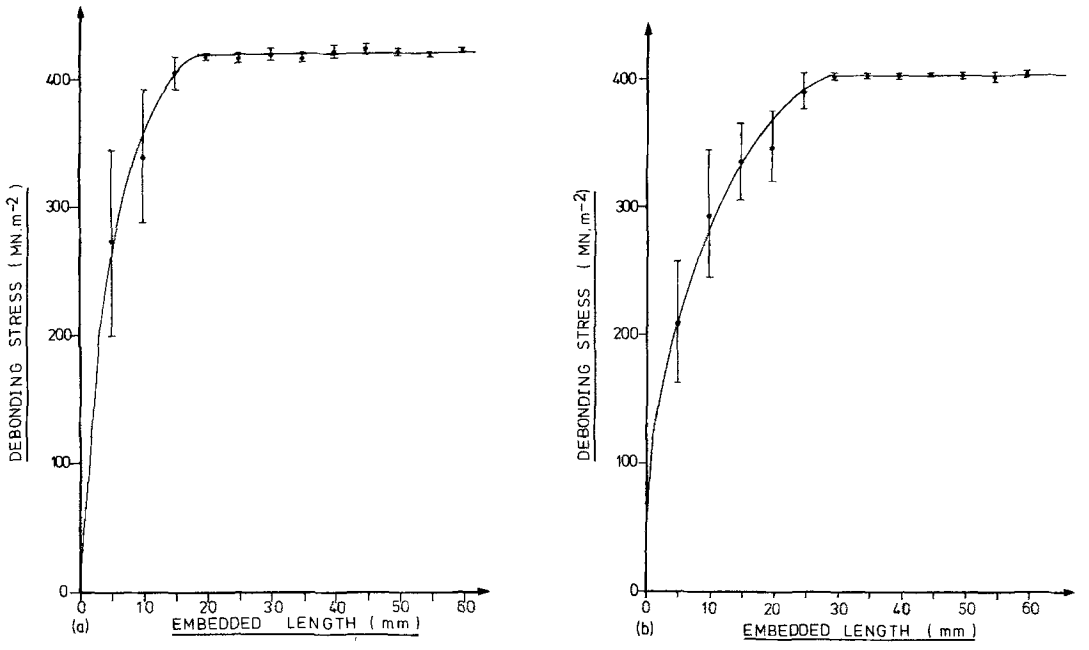

Figure 8 Debonding stress versus embedded length for (a) 0.5 mm diameter wire, (b) 1 mm diameter wire. Yield stress 400 MN m^{-2}.

required to achieve plateau debonding is 18 mm for the 0.5 mm diameter wire and 28 mm for the 1 mm diameter wire. Another estimate of the critical length can be obtained by extrapolating the dependence of debonding plateau length on embedded length. Fig. 9a and b shows this dependence, which is a direct representation of Equation 4 of the model. The slopes of the lines in Fig. 9 give values of 1.9% and 1.6% for the debonding strains of the 0.5 and 1.0 mm diameter wire, respectively, implying that the 1 mm diameter wire was slightly rougher. (X = 4 μm as opposed to 2.4 μm for the 0.5 mm diameter wire.) The intercepts of Fig. 9 give critical lengths of 15.5 and 22 mm for the 0.5 and 1 mm diameter wires, respectively, in fair agreement with the estimates from Fig. 8. The implied average shear stresses τ_{av} of 3.4 and 4.6 MN m^{-2}, respectively, compare

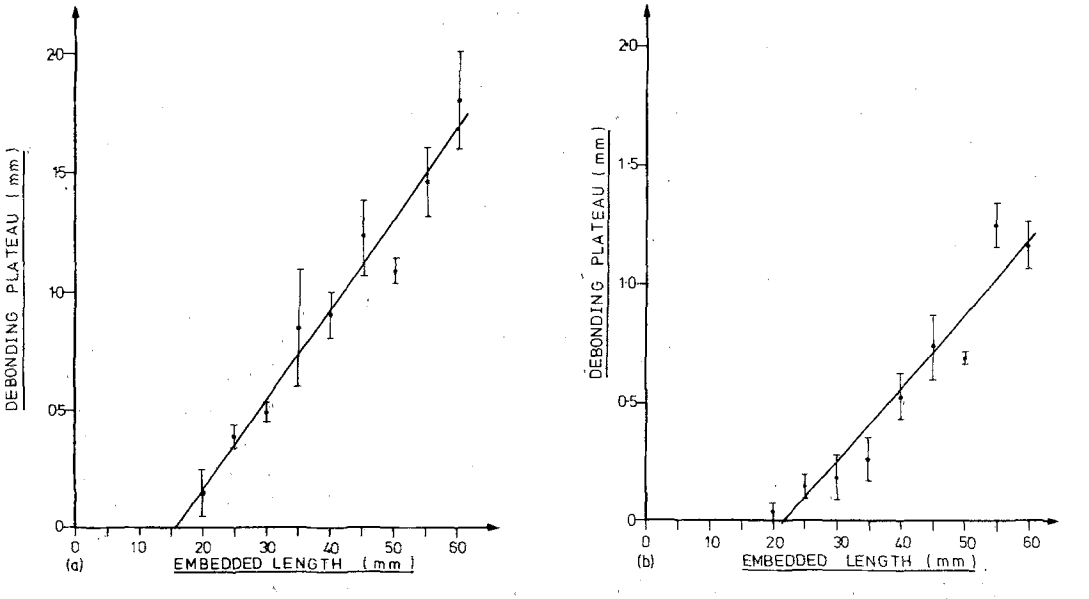

Figure 9 Debonding plateau length for (a) 0.5 mm diameter wire, (b) 1 mm diameter wire.

well with the value of 3.2 MN m^{-2} calculated for similar as-received wires from the dependence of debonding plateau on wire diameter.

The effect of embedded length on pull-out stress is shown in Fig. 10. The considerable scatter is to be expected from the fluctuations in pull-out stress already commented upon. The maximum stress attained during pull-out was taken to be the pull-out stress for Fig. 10. According to the model, the pull-out stress should remain constant for embedded lengths in excess of the critical length. The results, however, show a rising trend. This may be accounted for by random fluctuations in wire diameter, such that for a longer pull-out length the plug may be expected to encounter a more severe constriction in the matrix tunnel, leading to a higher maximum in pull-out stress. Below the critical length, elastic debonding occurs and the pull-out stress increases linearly with embedded length. (Strictly, elastic radial contraction of the wire causes the pull-out stress to increase less-than-linearly with embedded length, as shown by Takaku and Arridge [4], but in our case a linear approximation is adequate.) From the slopes of the initial straight lines, frictional shear stresses opposing pull-out of 2.3 and 2.4 MN m^{-2} are implied for the 0.5 and 1 mm diameter wires, respectively.

4.5. Effect of matrix-cement compared to resin

Results for nickel wires in a cement matrix are shown in Fig. 11a and b. For a sufficient embedded length, a debonding plateau is again observed at a stress somewhat in excess of the yield stress of the wire. The scatter in data was, in general, worse than it was for the resin matrix and, in particular, debonding plateau lengths were too scattered to give useful results. Fluctuations in stress during pull-out were more severe than was the case for the resin matrix, such that it was not felt possible to assign a single pull-out stress to a particular specimen.

For as-received wire (Fig. 11a) the critical lengths were approximately in the ratio of the wire diameters and were roughly twice the value for the same wires in resin. This indicates a poorer bond in the cement. The plateau debonding stress for the 0.5 mm wire was 407 MN m^{-2} as compared to 420 MN m^{-2} for the resin matrix. This difference is statistically highly significant and implies a smaller debonding strain in the cement matrix for the same wire. This is not directly explicable from the simple model but it may be the result of the cement matrix being more fragile or compactable than the resin, so that traction at the interface can be destroyed by the matrix asperities giving way when the radial contraction of the wire is smaller.

Nickel wire of 0.4 mm diameter, annealed in air and pulled to a yield stress of 250 MN m^{-2} showed a much shorter critical length (Fig. 11b). Improved bonding to the oxidized surface may explain this. The pull-out stresses were of a similar magnitude to the debonding stresses and the pulled-out wire

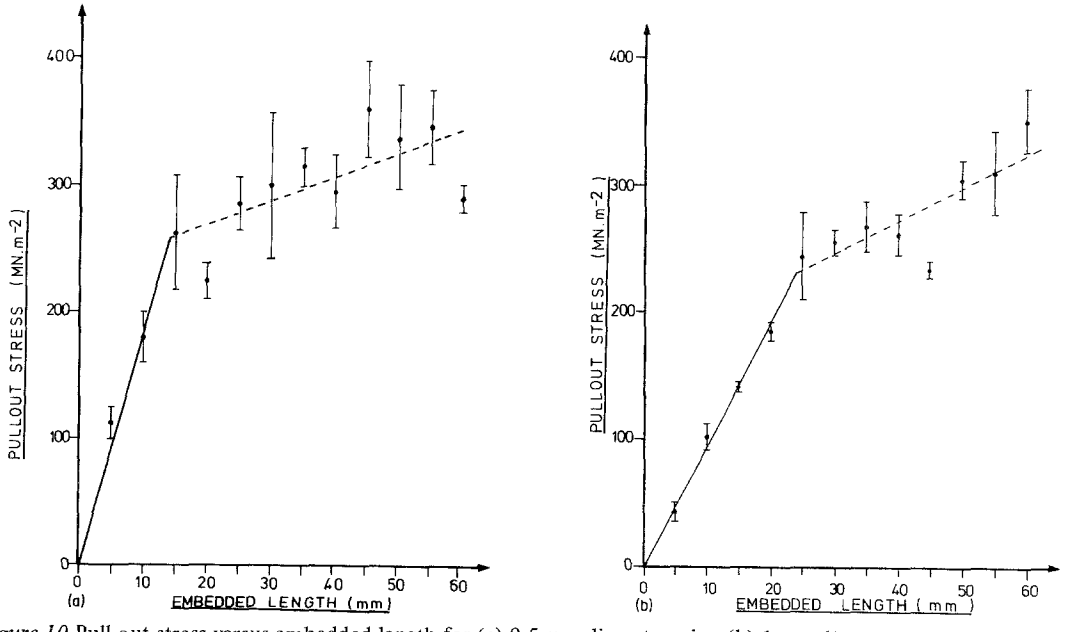

Figure 10 Pull-out stress versus embedded length for (a) 0.5 mm diameter wire, (b) 1 mm diameter wire.

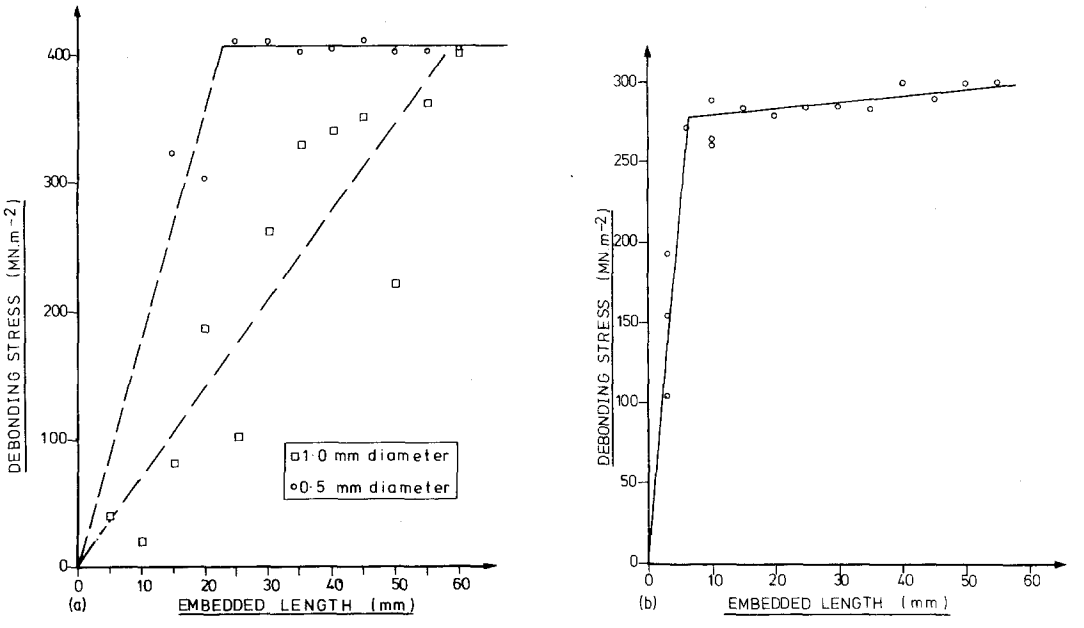

Figure 11 Debonding stresses for cement matrix, (a) wire annealed in argon/H_2, yield stress 400 MN m^{-2}, (b) wire annealed in air, yield stress 250 MN m^{-2}.

had particles of cement adhering to it. Talysurf traces showed that this wire was rougher than the as-received wire, and this, as well as its oxidized surface may be a factor in accounting for its improved performance. The origin of the slight increase in plateau debonding stress with increasing embedded length in these specimens is not understood.

4.6. Effect of wire orientation

As received wires were pulled to a yield stress of 400 MN m^{-2} and embedded in resin at various angles to the tensile axis. The propagation of a debonding front could be observed as for aligned wires, but for angles above 25° to the tensile axis, the wire failed before completion of debonding. For wires which debonded fully, the rise in debonding plateau stress with inclination of the wire is most rapid over the first 10° of inclination (Fig. 12). The pull-out stress is increased above the value for an aligned wire in a similar manner, consistent with previous work [1]. The behaviour of inclined wires can be included within the model by simply adding to the stress applied to wire at the crack face a contribution due to friction near the exit point where the wire turns into alignment with the applied stress. The propagation of the debonding front and the pull-out of a terminal plug appear qualitatively the same as in the case of aligned wires.

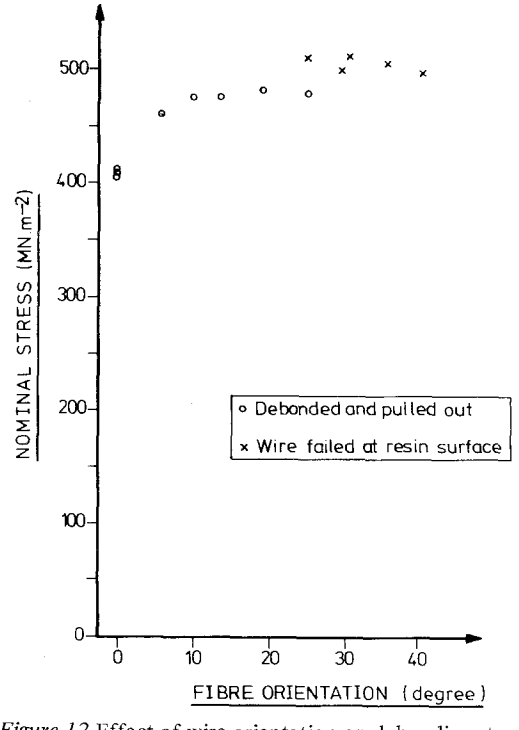

Figure 12 Effect of wire orientation on debonding stress.

5. Discussion

The experimental results satisfactorily support the

model of the debonding of a wire from a brittle matrix by the progression of a yielded zone along the wire and the pull-out of the wire by the withdrawal of a terminal plug of wire remaining in contact with the matrix, for both resin and cement paste matrices. The question remains to what extent this behaviour could be of benefit in real composites. One problem is whether the behaviour shown by our single-wire specimens would be reproduced during the propagation of a matrix crack in a mult-wire composite. A subsequent paper will show that this is, in fact, the case. We can then consider the most desirable behaviour of a single wire in debonding and pull-out for the purpose of interfering with crack propagation in a composite. This would be for the wire to reach, as rapidly as possible, a high stress as the crack opened, and to maintain that stress up to large displacements of the surfaces of the crack. If we consider first composites containing relatively short lengths of wire mixed randomly into the matrix, such as cement reinforced with chopped steel wire, the main difficulty will be in achieving a sufficiently short critical aspect ratio l_k/d. Because of mixing requirements, the largest aspect ratio of wire likely to be practicable [6] is ~ 100. The shortest critical aspect ratio achieved in this work was approximately 30, for air-annealed nickel in cement (Fig. 11b). If l is the actual wire length, only the fraction $(1 - l_k/l)$ of wires intersected by a crack would reach the debonding plateau stress. Assuming that the stress supported by the remainder varies linearly with embedded length, the debonding stress must be multiplied by an "efficiency factor" η, similar to that defined for brittle elastic fibres [7] to obtain the average stress supported, where

$$\eta = (1 - l_k/2l). \quad (8)$$

From Equation 6 the critical aspect ratio can be improved by increasing τ_{av}, an average of the shear stresses transmitted on either side of the debonding front. Improving the bond strength and increasing the wire roughness may be expected to enhance these stresses. It is notable that although the strength of bonding of the wire has no influence on the plateau debonding stress it is of great importance in determining the critical aspect ratio. Increasing the residual shrinkage stress exerted by the matrix on the wire may also increase τ_{av} and reduce l_k.

In the case of composites containing long or continuous wires, the benefits of the model could be more easily realized. It would be important to adjust the surface roughness of the wire to maximize the debonding stress, debonding strain and pull-out stress without increasing the roughness so far that the wire fractured. In our experiments, the largest debonding strain achieved was 8%, at a roughness obtained by pulling the wire to fracture. It will be difficult to achieve debonding strains as large as those obtained by Millman and Morley [8] ($\sim 20\%$) in "dupile" elements consisting of a metal tube containing a core, such that the core arrests the necking down of the tube which accompanies debonding. However, the debonding and pull-out behaviour of simple wires in our experiments is qualitatively similar to that of the more complex "dupile" elements.

6. Conclusions

Ductile wires embedded in a brittle matrix, with an embedded length exceeding a critical value may debond from the matrix at a stress independent of the embedded length and determined by the yield stress and work-hardening rate of the wire and its surface condition, particularly its roughness. A plastic strain then occurs during debonding, which for a given surface condition of wire, varies inversely as the wire diameter. The pull-out of a wire which has debonded in this manner occurs at a constant stress independent of embedded length but dependent on the surface condition of the wire, until the embedded length has fallen to a critical value. These effects are explained by a simple model in which debonding is accompanied by a plastic contraction of the wire radius sufficient to overcome its surface roughness and take the wire out of contact with the matrix.

Because of the substantial critical length of wire needed to produce these effects, they are most likely to be of practical significance in composites containing long or continuous wires.

Acknowledgements

The financial support of the Science Research Council is acknowledged. The authors are grateful to L.A. Owen for careful technical assistance.

References

1. J. MORTON and G. W. GROVES, *J. Mater. Sci.* **11** (1976) 617.

2. J. P. OUTWATER and M. C. MURPHY, Paper 11c, 24th Annual Technical Conference S.P.I. Reinforced Plastics Division (1969).
3. P. LAWRENCE, *J. Mater. Sci.* 7 (1972) 1.
4. A. TAKAKU and R. G. C. ARRIDGE, *J. Phys. D.* **6** (1973) 2038.
5. J. MORTON and G. W. GROVES, *J. Mater. Sci.* **10** (1975) 170.
6. R. N. SWAMY and P. S. MANGAT, *Concrete* 8 (1974) 34.
7. V. LAWS, *J. Phys. D. Appl. Phys.* **4** (1971) 1737.
8. R. S. MILLMAN and J. G. MORLEY, *J. Phys. D.* 8 (1975) 1065.

Received 12 May and accepted 17 July 1978.